JCTC Journal of Chemical Theory and Computation

Article

pubs.acs.org/JCTC

A Novel Approach for Deriving Force Field Torsion Angle Parameters Accounting for Conformation-Dependent Solvation Effects

Marie Zgarbová,[†] F. Javier Luque,[‡] Jiří Šponer,[§,∥] Michal Otyepka,[†] and Petr Jurečka*[,†]

[†]Regional Centre of Advanced Technologies and Materials, Department of Physical Chemistry, Faculty of Science, Palacky University, 17. listopadu 12, 77146 Olomouc, Czech Republic

[‡]Department de Fisicoquímica and Institut de Biomedicina (IBUB), Facultat de Farmàcia, Universitat de Barcelona, Avgda Diagonal 643, Barcelona 08028, Spain

[§]Institute of Biophysics, Academy of Sciences of the Czech Republic, Královopolská 135, 612 65 Brno, Czech Republic

[∥]CEITEC - Central European Institute of Technology, Masaryk University, Campus Bohunice, Kamenice 5, 625 00 Brno, Czech Republic

Supporting Information

ABSTRACT: A procedure for deriving force field torsion parameters including certain previously neglected solvation effects is suggested. In contrast to the conventional in vacuo approaches, the dihedral parameters are obtained from the difference between the quantum-mechanical self-consistent reaction field and Poisson−Boltzmann continuum solvation models. An analysis of the solvation contributions shows that two major effects neglected when torsion parameters are derived in vacuo are (i) conformation-dependent solute polarization and (ii) solvation of conformation-dependent charge distribution. Using the glycosidic torsion as an example, we demonstrate that the corresponding correction for the torsion potential is substantial and important. Our approach avoids double counting of solvation effects and provides parameters that may be used in combination with any of the widely used nonpolarizable discrete solvent models, such as TIPnP or SPC/E, or with continuum solvent models. Differences between our model and the previously suggested solvation models are discussed. Improvements were demonstrated for the latest AMBER RNA χ_{OL3} parameters derived with inclusion of solvent effects in a previous publication (Zgarbova et al. *J. Chem. Theory Comput.* **2011**, *7*, 2886). The described procedure may help to provide consistently better force field parameters than the currently used parametrization approaches.

1. INTRODUCTION

Molecular modeling provides valuable insights into the structure, dynamics, and function of nucleic acids. However, the quality of the results derived from molecular dynamics (MD) simulations is heavily dependent on the accuracy of the empirical force fields employed.[1−3] One of the crucial components of any empirical force field is the torsion space parametrization. The dihedral profiles modulate the relative stability of various biomolecular conformers (or folds) and the kinetics of the transitions between them. Atomic-resolution structures reveal that nucleic acids can adopt numerous, distinct combinations of backbone angles (conformational classes) that influence their topology, and hence their interactions with other molecules.[4,5] For instance, the BI/BII equilibrium, characterized as correlated substates of the ε/ζ backbone angles, putatively plays a key role in the recognition of DNA by proteins.[5]

In order to perform well in simulations, force fields should be capable of correctly reflecting the very delicate balance between various backbone conformations of nucleic acids. This is not a trivial problem, since the force fields have very simple functional forms and the dihedral terms are used to implicitly compensate for many energy terms. Current empirical torsion parameters generally describe the most common nucleic acid forms in short simulations starting from experimentally characterized structures quite well. These include the frequently studied double helical DNA. The good performance for these common structures is partially because they were considered during the force fields' development. Unfortunately, however, the torsion parameters may be inadequate for less common structures. Therefore, there has been a long history of readjustment of most force fields' torsion spaces.[6−11,3] For instance, in the nucleic acid force field family based on the very successful parametrization of Cornell et al.,[12] the torsions relating to sugar pucker,[6,13] χ,[6,3] and α/γ[9] dihedrals have all been officially revised in recent years, some of them several times. Two of the revisions are critical refinements for stabilizing MD simulations of canonical duplexes over prolonged time scales and preventing irreversible structure degradation.[9,3] It should be noted that any attempt to tune the dihedral profiles must be accompanied by extensive testing in simulations.

The frequent readjustments of torsion parametrizations show that developing torsion parameters is difficult and raises profound questions about sources of errors and biases in the parametrization procedures. Some errors may be introduced by inaccuracies in the individual vdW parameters, bending terms, electrostatic components, etc., which are often system-dependent and require case-by-case solutions. In addition, systematic

Received: March 8, 2012
Published: August 21, 2012

biases may be introduced by the approximations used during parameter development. These are of particular interest to us here.

In this article, we focus on the QM-based development of torsion parameters for molecular mechanics (MM). Specifically, we ask whether a systematic bias may be introduced by deriving the torsion parameters in vacuo. Usually, QM dihedral energy profiles are obtained in vacuo and used as targets for the torsion fitting. The dihedral angle contributions are calculated as a difference between the vacuum QM energy profiles ($E^{QM,vac}$) and vacuum MM energy profiles, where the MM energy is calculated without considering the contribution of the calibrated dihedral ($E_{-\chi}{}^{MM,vac}$, see also Methods, below). For instance, if we are interested in the torsion angle χ, the dihedral torsion contribution, $E_{dih,\chi}{}^{vac}$, can be obtained from eq 1:

$$E_{dih,\chi}{}^{vac} = E^{QM,vac} - E_{-\chi}{}^{MM,vac} \quad (1)$$

This difference is evaluated for a set of χ angles and then fitted using a cosine series (the corresponding fitted torsion parameters are denoted as χ_{vac} in the following). In this way, many complex effects that are not described at the MM level are elegantly incorporated into the MM parameters. For instance, the internal energy changes due to charge redistribution within the molecule, which are present in the QM calculation, are implicitly included. Note that this procedure also partially corrects for errors introduced by the conformation-independent (fixed) charges in MM, because it includes the differences between the inaccurate fixed-charge Coulombic interactions in MM and the accurate QM values.

However, MD simulations are usually carried out on molecules in aqueous solution. Consequently, parameters derived for molecules in a vacuum may not be fully adequate. This issue is rarely discussed, and the magnitude of the resulting error has not been investigated in depth. It is commonly argued that such investigations are unnecessary because the torsion parameters often need empirical adjustment in any event due to the numerous other approximations that are used. As such, if the parameters derived for molecules in a vacuum do not provide reasonable results for molecules in aqueous solution, they will be empirically adjusted so as to reproduce some experimental observable. However, there are also a number of works that consider solvation, at least at some stage of the process of parameter development.[14,15] For instance, Duan et al.[15] refitted the main-chain torsion parameters for proteins[15] with the MP2/cc-pVTZ/IEFPCM data taken as a reference. In this approach, however, some portion of the conformation-dependent solvation energy (namely, the $\Delta G^{upSu-Sv}$ contribution detailed below) is double-counted, because the torsion parameters are fitted to data including the full QM solvation energy and subsequently used in MD simulations with the explicit solvation model. It should be noted that in some cases the errors resulting from such double counting may be small, without substantially affecting the overall force field performance. Nevertheless, these works demonstrate the growing interest in including the solvent effects into parametrization efforts.

Here, we explore an alternative strategy for systematically correcting for the bias introduced by deriving torsion parameters in vacuo (recently, we used this method to derive glycosidic torsion parameters χ_{OL3},[3] but without providing a detailed justification). The discrete solvent models used in MD simulations (e.g., TIP3P) account for much of the solvation energy but systematically neglect some important solvation contributions (see below). Therefore, it would be desirable to somehow include these effects implicitly in the parametrization, while avoiding double counting of the same solvation contributions. One way of including the missing solvation effects in the dihedral term, $G_{dih,\chi}{}^{solv}$, is illustrated in eq 2.

$$\begin{aligned} G_{dih,\chi}{}^{solv} &= E^{QM,vac} + \Delta G^{solv,QM/SCRF} \\ &\quad - (E_{-\chi}{}^{MM,vac} + \Delta G^{solv,MM/PB}) \\ &= E_{dih,\chi}{}^{vac} + \Delta\Delta G^{solv,QM-MM} \end{aligned} \quad (2)$$

In this equation, $\Delta G^{solv,QM/SCRF}$ stands for the solvation free energy determined using any self-consistent reaction field method (SCRF), i.e., a continuum model with self-consistently treated polarization, such as MST,[16−19] IEFPCM,[20−22] COSMO,[23−25] or SMD.[26] $\Delta G^{solv,MM/PB}$ represents the Poisson−Boltzmann (PB) solvation energy determined using a given set of fixed atomic charges (but other polarized continuum solvation models, such as COSMO, may be used as well). Thus, the target for fitting is not the in vacuo energy ($E^{QM,vac}$) as in eq 1 but the in vacuo energy plus the difference between the MM and QM continuum solvation energies, $E^{QM,vac} + \Delta\Delta G^{solv,QM-MM}$ (the corresponding fitted torsion parameters are denoted as χ_{wat} in the following). Note that the terms on the right-hand side of eq 2 are different in nature (free energy vs energy), and so referring to the result in terms of free energy (G) is somewhat inaccurate. It is important to remain mindful of the term's mixed origin.

Equation 2 differs from eq 1 only in the difference between the QM and MM solvation energies, $\Delta\Delta G^{solv,QM-MM}$. This term could potentially be incorporated into the parametrization of the χ torsion. To this end, we analyze the origin of this term by splitting it into its individual components and estimating the impact of each one. Then, we also investigate whether including this term in force field parametrization could lead to improvements in MD simulations of molecules in aqueous solution.

As a model system for our study, we focus on the torsion angle χ in cytosine deoxyribonucleoside (Figure 1). The dihedral angle χ describes the relative orientation of the nucleotides and sugar moieties in DNA and RNA and strongly influences many structural parameters of nucleic acids, such as their helical twist, propeller twist, groove widths, etc. It also affects the propensities of the DNA duplex to populate its A

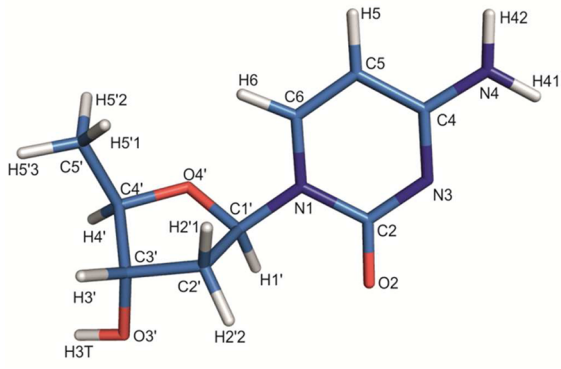

Figure 1. Model of cytosine deoxyribonucleoside. The torsion angle χ (O4′−C1′−N1−C2) describes the relative orientation of the nucleotide and sugar moieties in DNA and RNA.

dx.doi.org/10.1021/ct3001987 | J. Chem. Theory Comput. 2012, 8, 3232−3242

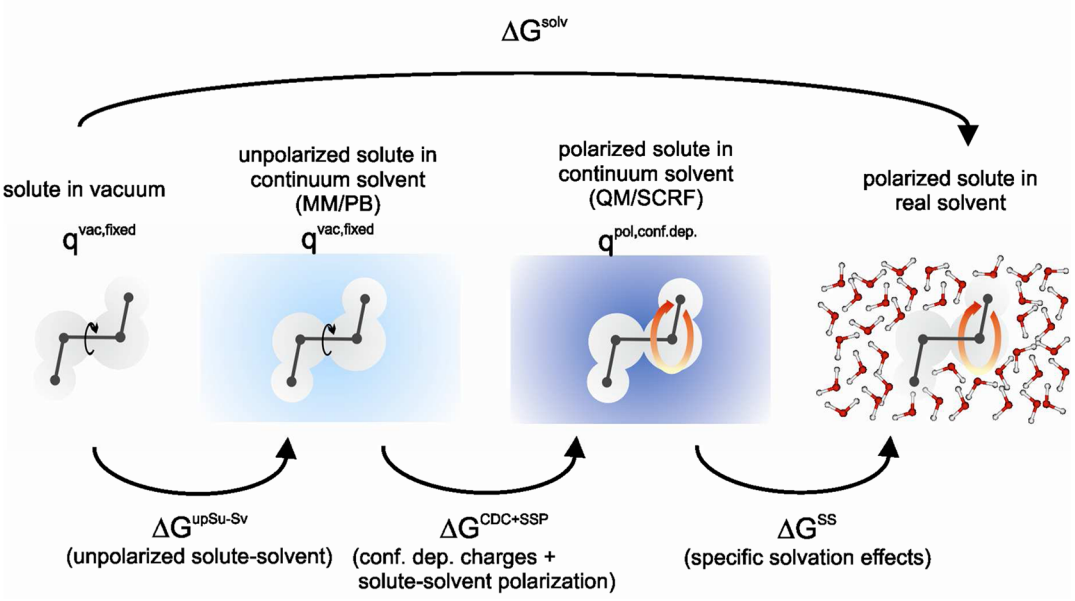

Figure 2. Decomposition of the solvation energy. The total solvation energy, ΔG^{solv}, is decomposed into three components: (i) $\Delta G^{upSu-Sv}$, the interaction of the unpolarized solute (vacuum charge q^{vac}) with the continuum solvent; (ii) $\Delta G^{CDC+SSP}$, the contribution from solute−solvent polarization (SSP) and the conformation dependence of point charges (CDC), where $q^{pol,conf.dep}$ represents polarized and conformation dependent charges; and (iii) the remaining specific solvation effects of real discrete solvent, ΔG^{SS}. The darkness of the blue indicates the strength of the solvent polarization and red arrows indicate the conformation dependence of point charges.

and B forms. The χ torsion parameters are among the most frequently revised nucleic acid force field parameters[12,6,7,27,28,10,11,3] due to their major impact on simulations.[29,1,30,31]

The solvation approach presented in this paper is not only physically meaningful but is also justified by our recent successful reparameterization of the χ torsion for RNA, χ_{OL3},[3] which has been done with the inclusion of solvent effects. The Zgarbova et al. χ_{OL3} correction was shown to stabilize RNA simulations by preventing degradation of RNA structures into so-called "ladder-like" geometries. Moreover, it provides major improvements in simulations of A-RNA, UNCG, and GNRA RNA hairpins;[1,3] reverse kink-turns;[31] and other systems (to be published). These parameters have been incorporated into the ff10 force field in the Amber program package,[32] where they are denoted χ_{OL3} (the numbering used during their development) and are identical to the χ_{OL} parameters discussed in the original work.[3] Note that these parameters were made available in the Supporting Information for our benchmark study on RNA tetraloops[1] prior to publication of the original work.[3]

The discussion is organized as follows. First, we consider the partitioning of the total solvation energy into various physical contributions. Then, we examine which of these contributions are present in various solvation models—PB, Semiclassical-Continuum approach,[33] SCRF, and discrete MM models. After that, the magnitude of the major effects contributing to $\Delta\Delta G^{solv,QM-MM}$ is estimated, and the origin of this term is discussed. Finally, we discuss the viability and benefits of using our new approach to model solvent effects.

2. METHODS

Geometries. A relaxed χ scan with 10° increments was performed using the PBE functional[34] and the 6-311++G(3df,3pd) atomic basis set[35−38] (hereafter denoted LP for the sake of brevity) with the COSMO solvent model[23] in the TurboMole 6.3 software package.[39,40] The sugar pucker was maintained close to the C2′-endo configuration by freezing the τ_3 angle (C2′−C3′−C4′−O4′) at 25.7° (the optimal value for a fully relaxed structure in its *anti* minimum). These optimal geometries were used for all calculations in this study for the sake of consistency and to avoid mixing energy changes due to geometric relaxation with electronic effects. Using the same geometries for both MM and QM calculations is, however, necessary only for the analysis presented in this article. In force field development, geometries were optimized independently at MM and QM levels.[3]

Solvation Energies. Several approximations were used to simplify the investigation into the impact of solvation effects on the torsion energy. Only the electrostatic component of the solvation energy was considered; i.e., nonpolar contributions (dispersion, repulsion, and cavitation) were omitted. This omission should not affect our main conclusions, because the electrostatic component usually dominates the solvation of polar molecules. Moreover, the nonpolar solvation contributions would nearly cancel out in our derivations as they are meant to be described by the solvent models used in MD simulations (see below). For consistency, the same radii were used in all our calculations (QM/SCRF, MM/PB, and semiclassical); for more details, see the Results and Discussion. The same radii were also used for the RESP calculations (see below).

In the QM calculations, solvation energies were calculated using the COSMO continuum solvent model.[23] COSMO has been carefully parametrized using a large set of solvation free energies and has proven to provide reliable estimates of the hydration free energy in the SAMPL contest.[41,42] Calculations were performed at the PBE/LP level of theory and using the optimized default set of vdW radii implemented in the TURBOMOLE 6.3 software suite.[39,40] The COSMO solvation energies were decomposed using the Gaussian 03 program[43] (SCRF = CPCM) at the same level of theory.

MM/PB calculations were performed using the code implemented in AMBER10,[44] using the default radii from the TURBOMOLE package for consistency (see above). The grid spacing was set to 0.1 Å, the solvent permittivity to 78.4, and the solvent probe radius to 1.3 Å. Only the electrostatic part of the solvation energy was considered; the nonpolar solvation energy in the single-point calculations with the continuum models was disregarded. Four different charge sets were used (see below).

Semiclassical-continuum (SC)[33] solvation energies were computed using a locally developed FORTRAN code with radii taken from the TURBOMOLE code (see above). The SC approach[33] is based on first-order perturbation treatment of the linear response approximation for the solvent effect.[45] The method relies on the use of two sets of partial charges: one for the solute in vacuo ($q^{\mathrm{vac,conf.dep}}$—see below) and the other for the fully polarized solute in solution ($q^{\mathrm{pol,conf.dep}}$—see below). This makes it possible to inexpensively calculate the contribution to the solvation energy from the solute polarization.

Charge Sets. Several calculations were performed using the following four charge sets.

- q^{ff94}: standard fixed point charges taken from ff94.[12] The charges of the H5′1, H5′2, and H5′3 hydrogens were specified as being identical so that the total charge of the molecule was zero.
- $q^{\mathrm{vac,fixed}}$: PBE/LP RESP charges derived in vacuo for a single conformation taken as the global anti minimum (χ = 240°).
- $q^{\mathrm{vac,conf.dep}}$: PBE/LP RESP charges derived in vacuo for each value of the χ angle (conformation) separately.
- $q^{\mathrm{pol,conf.dep}}$: PBE/LP RESP charges derived using the CPCM solvent model with ε = 78.4 for each value of the χ angle (conformation) separately.

RESP charges[46] were derived using the antechamber program. Gaussian 03[43] was used to calculate the QM electrostatic potential with the IOP(=6/33=2,6/41=1,6/42=10) option and radii taken from TurboMole (see above). More details of the specific calculations performed with the different charge sets are given in the Results and Discussion.

3. THEORETICAL BACKGROUND

3.1. Decomposition of the Solvation Energy. The transfer of a solute from a vacuum to a solution can be represented by three hypothetical steps (Figure 2), chosen to relate the corresponding solvation contributions to the results provided by specific solvation calculations—PB or SC models in MM (MM/PB or MM/SC), self-consistent reaction field models in QM (QM/SCRF), and discrete solvent models used in MD, such as TIPnP.

The individual steps in the decomposition process for isolating the individual components of the solvation energy are as follows:

(i) First, the conformation-independent vacuum charge distribution of the solute is solvated by a continuum model. The contribution of the interaction between the unpolarized (vacuum) solute charge distribution and the solvent ($\Delta G^{\mathrm{upSu-Sv}}$) can be estimated from the MM/PB calculations, in which the fixed force field point charges are used. It is worth noting that the MM charges used in nonpolarizable force fields are intentionally prepolarized and differ from the in vacuo charges. However, here, we start with the in vacuo charges and relate the results to the prepolarized charges at a later stage.

(ii) Second, the charge distribution of the solute is polarized by the solvent (ΔG^{SSP}) and is allowed to relax to suit the solute conformation (ΔG^{CDC}). The corresponding contribution ($\Delta G^{\mathrm{CDC+SSP}}$; conformation charge dependence + solute polarization) is accounted for in QM-SCRF methods such as IEFPCM or COSMO. They may also be included by using MM/SC model as described in ref 33.

(iii) Third, the continuum representation of the solvent is replaced with an explicit treatment of discrete solvent molecules, which generates additional effects (collectively called "specific solvation") that are collectively denoted by ΔG^{SS}. Some of these additional effects are captured relatively well by classical solvent models such as TIPnP, notably effects relating to the size and topology of the solvent molecules, such as the incorporation of bridging water molecules, the diffusion of single solvent molecules into solute cavities, orientation polarization, and so on. However, other effects must be modeled by explicit QM solvent molecules, such as specific orbital interactions, charge transfer, or any interaction with partly covalent character.

The sum of the contributions shown in Figure 2 gives the total solvation energy, ΔG^{solv} (eq 3), if we assume that the nonelectrostatic terms appear in the last term, ΔG^{SS}. This choice is arbitrary and does not affect the conclusions drawn in this work.

$$\Delta G^{\mathrm{solv}} = \Delta G^{\mathrm{upSu-Sv}} + \Delta G^{\mathrm{CDC+SSP}} + \Delta G^{\mathrm{SS}} \quad (3)$$

Table 1 shows which of the solvation components described above (i to iii) are accounted for by various solvent models.

Table 1. Overview of the Solvation Components Covered by Different Solvent Models (See Also Figure 2)

model	unpolarized solute−solvent $\Delta G^{\mathrm{upSu-Sv}}$	solute−solvent polarization + conformation charge dependence $\Delta G^{\mathrm{CDC+SSP}}$	specific solvation ΔG^{SS}
MM/PB ($\Delta G^{\mathrm{solv,MM/PB}}$)	yes	no[a]	no
QM/SCRF ($\Delta G^{\mathrm{solv,QM/SCRF}}$)	yes	yes	no
MM/Discrete solv ($\Delta G^{\mathrm{solv,MM/D}}$)	yes	no[a]	yes[b]

[a]Some portion of these effects may be included in the MM solvation, albeit implicitly and inaccurately, by using prepolarized charges (ΔG^{SSP}) and multiconformation RESP fitting (ΔG^{CDC}). [b]Only a fraction of the specific solvent (SS) effects is included in MM models. Some SS effects can be described only at the QM level.

Note that the decomposition is somewhat idealized. For instance, the MM/PB and discrete MM solvation energies may implicitly include some portion of the solute polarization, since they use prepolarized charges and are empirically parametrized to reproduce experimental data. The approximations made in this simple decomposition scheme are discussed later in the text.

From the data presented in Table 1, it is apparent that none of the available solvent models cover all of the effects involved in solvation (eq 3). While the MM/PB and QM/SCRF models

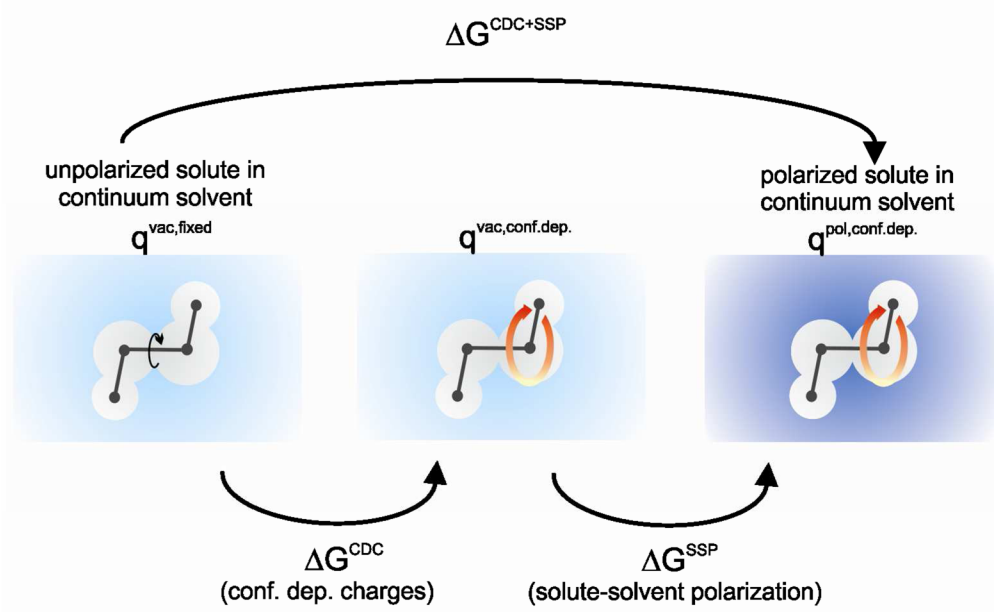

Figure 3. Decomposition of the difference between classical MM/PB solvation (left) and QM/SCRF solvation (right). The conformation charge dependence (ΔG^{CDC}, indicated by the red arrows) and solute−solvent polarization (ΔG^{SSP}, indicated by darkness of the blue coloration) are incorporated stepwise.

neglect specific solvation effects, discrete MM models in nonpolarizable force fields do not explicitly include solute polarization or the conformation charge dependence. However, by combining results from all three models, one can obtain an estimate of the total solvation energy according to eq 4:

$$\Delta G^{solv} \approx \Delta G^{solv,MM/D} + \Delta G^{solv,QM/SCRF} - \Delta G^{solv,MM/PB} = \Delta G^{solv,MM/D} + \Delta\Delta G^{solv,QM-MM} \quad (4)$$

The $\Delta G^{solv,MM/D}$ term represents classical solvation using a discrete solvent model such as TIP3P, TIP4P, or SPC/E and is present in any MD simulation with discrete solvent molecules. On the other hand, the $\Delta\Delta G^{solv,QM-MM}$ term is not explicitly included in simulations with classical (nonpolarizable) force fields. One way of adding this term to classical simulations is to incorporate it into the torsion parameters via eq 2. Then, when performing an MD simulation using a discrete solvent model, the main portion of the solvation energy is covered by this discrete solvent model, and the effects that are absent in the force field description, $\Delta G^{CDC+SSP}$, are provided by the torsion term.

3.2. Origins of the Difference between QM/SCRF and MM/PB Solvation Models. In this section, we focus on the second step in Figure 2, which covers differences between solvation with the QM/SCRF and MM/PB models ($\Delta\Delta G^{solv,QM-MM}$), stemming from the contributions related to the solute polarization, ΔG^{SSP}, and the solvation of conformation-dependent charges, ΔG^{CDC}. In order to separate these two effects, we can imagine the transition between MM/PB and QM/SCRF models as being performed in two consecutive steps as shown in Figure 3. In the first step, the fixed charges are allowed to change with the conformation in vacuo, and the solvent reacts to the conformation-dependent vacuum charges. In the second step, the charges are further polarized by the solvent, which reacts to the new polarized conformation-dependent charges.

Solvent Response to Conformation-Dependent Charges. Conformational changes affect the charge distribution in the solute. Consequently, both the internal (intramolecular) solute energy and the solute−solvent (intermolecular) interactions change. These changes are denoted by ΔG_{Su}^{CDC} and ΔG_{Sv}^{CDC}, respectively. Such changes are not reflected in classical nonpolarizable force fields, as the electronic distribution is represented by a set of fixed point charges ($q^{vac,fixed}$), which is a well-known drawback of these methods.[47] Clearly, better results could be achieved if each conformation were represented by its own set of charges ($q^{vac,conf.dep}$). Here, it is important to realize that fixed charges and conformation-dependent charges generate different solvent responses. It is just the corresponding change due to conformation-dependent charges ($\Delta G^{CDC} = \Delta G_{Su}^{CDC} + \Delta G_{Sv}^{CDC}$) that is our main concern here. Because ΔG^{CDC} is naturally included in QM/SCRF calculations but is absent in MM/PB calculations with fixed charges (or in MM simulations with explicit solvent), it is likely to be an important component of any differences between the two models ($\Delta\Delta G^{solv,QM-MM}$).

Note that the MM/PB solvation energy itself is inherently conformation-dependent, because the relative orientation of the fixed charges (and thus the solvation energy) changes upon rotation of the torsion angle. However, the ΔG^{CDC} term, as defined here, does not include this component of the conformation-dependent solvation energy but only the contribution from the differential solvation of the fixed and conformation-dependent point charges.

Solute Polarization. When immersed in a solvent, the solute becomes polarized, and its charge distribution changes. Consequently, both the internal energy of the solute and the solute−solvent interactions change. These changes are referred to as ΔG_{Su}^{SSP} and ΔG_{Sv}^{SSP}, respectively. While the solute−solvent polarization is contained in the QM/SCRF solvation energies, it is not included in MM calculations with nonpolarizable force fields. Thus, the contribution from solute polarization ($\Delta G^{SSP} = \Delta G_{Su}^{SSP} + \Delta G_{Sv}^{SSP}$) also contributes to the difference between the QM/SCRF and MM results, $\Delta\Delta G^{solv,QM-MM}$. Note that solute polarization in MM is often

approximated implicitly by using prepolarized charges of some kind, e.g., HF/6-31G* RESP or Duan et al. charges.[15] However, such approaches do not account for conformation-dependent changes in solute polarization because the point charges are fixed.

As mentioned before, both ΔG^{SSP} and ΔG^{CDC} have intra- and intermolecular components. It would be interesting to obtain a detailed breakdown of how the different intra- and intermolecular components of solvation are taken into account when the torsion parameters are derived in vacuo (according to eq 1) and in solvent (according to eq 2). Table 2 lists all of the relevant components for the two parametrizations.

Table 2. Torsion Energy Components That Are Included When Torsion Parameters Are Derived in Vacuo (eq 1) and in Solvent (eq 2) (See Also Figure 3)

	torsion derived in vacuum (eq 1)		torsion derived in solvent (eq 2)	
contribution to solvation	internal energy of solute	interaction with solvent	internal energy of solute	interaction with solvent[a]
conformation dependence of charges (CDC)	yes[b] ΔE_{Su}^{CDC}	no	yes[b] ΔG_{Su}^{CDC}	yes ΔG_{Sv}^{CDC}
solute–solvent polarization (SSP)	no	no	yes[b] ΔG_{Su}^{SSP}	yes ΔG_{Sv}^{SSP}

[a]When using eq 2 to derive parameters, the ΔG_{Sv}^{CDC} and ΔG_{Sv}^{SSP} terms are included in the torsion parameters despite being intramolecular terms. See also the discussion in the Theoretical Background section. [b]Only a fraction of the intramolecular interactions is included, depending on the size of the model used during parameter development.

Let us first consider the terms in the first row of Table 2, which describe effects relating to the conformation dependence of the charge distribution. When torsion parameters are derived in vacuo, the difference between the QM and MM intramolecular electrostatic energies becomes incorporated into the derived torsion. Thus, although the point charges used in the force field are fixed, the intramolecular effects due to conformation charge dependence are included in the resulting parameters (ΔE_{Su}^{CDC}). The extent to which these intramolecular interactions are included depends on the size of the model, but relatively small models are usually sufficient because torsion energies are usually most sensitive to short-range contributions. On the other hand, interactions with the solvent are determined using fixed point charges, and so the solvation aspects of the conformation dependence of the charge distribution are not included. When using eq 2, the solvent response to the conformation dependent charge distribution is described by the QM/SCRF calculation, and so both ΔG_{Su}^{CDC} and ΔG_{Sv}^{CDC} are included in the resulting torsion parameters. Similar arguments also apply to solute–solvent polarization. While SSP effects are not accounted for in the in vacuo derived torsion, both the ΔG_{Su}^{SSP} and ΔG_{Sv}^{SSP} terms are included in the torsion derived in solvent via the $\Delta\Delta G^{solv,QM-MM}$ term (eq 2), in full analogy to the way the conformation-dependent internal energy of solute in a vacuum is included in the in vacuo derived parameters.

4. RESULTS AND DISCUSSION

In this section, we first examine the magnitude of the solvation-related effects mentioned above and discuss to what extent they can explain the differences between the QM/SCRF and MM/PB solvation models. We then discuss the utility of including these effects when deriving torsion parameters.

4.1. Magnitude of the Effects Absent from the in Vacuo Parameterization. Let us first look at the χ torsion profile in cytosine deoxyribonucleoside. Figure 4 shows the reference QM/SCRF (PBE/LP/COSMO) torsion profile and the MM/PB torsion profile calculated using the χ parameters derived in vacuo (χ_{vac}; full and dashed black lines, respectively). All curves are offset relative to the energy for χ = 210°, corresponding to the *anti* region in A-RNA. This figure is shown to highlight the difference between the performance of MM/PB calculations using χ_{vac} and those using χ parameters derived on the basis of QM/SCRF data for the molecule in solution. The difference between the results obtained with the two methods, $\Delta\Delta G^{solv,QM-MM}$, is plotted in red. For comparison with torsion profiles in vacuo and more discussion of the solvent effects on the profile shapes, see Figure S1 in the Supporting Information and our previous work.[9]

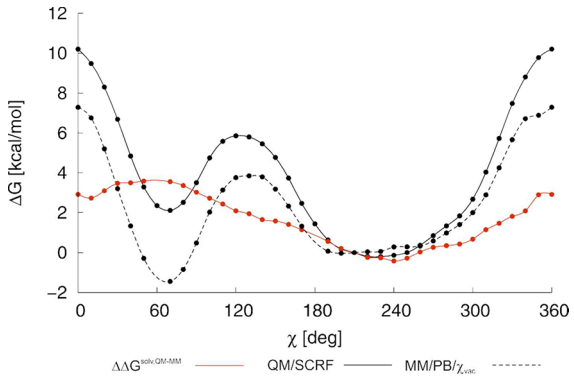

Figure 4. χ torsion profiles for cytosine deoxyribonucleoside obtained using the reference QM/SCRF PBE/LP method (solid black line) and MM/PB with χ torsion parameters derived using the same method in vacuo (χ_{vac}, dashed black line). For comparative purposes, the difference between the two profiles, $\Delta\Delta G^{solv,QM-MM}$, is also plotted in red. All curves are offset relative to the energy for χ = 210° (corresponding to the *anti* region in A-RNA).

The main purpose of Figure 4 is to show that the term $\Delta\Delta G^{solv,QM-MM}$, which can be viewed as a measure of the error due to the use of in vacuo derived parameters, makes a substantial contribution to the torsion profile. Indeed, the amplitude of this term (almost 4 kcal/mol) is comparable to the amplitude of the χ torsion potential *per se* (about 10 kcal/mol). Notably, it affects the relative energies of the most important regions on the χ torsion potential: the *anti* region around 210°, the *syn* region around 75°, and the barrier heights. In some cases, neglecting effects of this magnitude may have substantial consequences for MD simulations performed using such parameters.[3]

4.2. Magnitude of the Solvent Response to Conformation Charge Dependence. The effect of conformation charge dependence on the solvation energy can be estimated by performing force field calculations with two different charge sets: one that is conformation-independent ($q^{vac,fixed}$) and another that is conformation-dependent ($q^{vac,conf.dep.}$; for more details on charge derivation see Methods), in a continuum solvent model. For instance, in the PB continuum model, the ΔG_{Sv}^{CDC} term can be estimated according to eq 5.

$$\Delta G_{Sv}^{CDC} = \Delta G^{solv,MM/PB}(q^{vac,fixed}) - \Delta G^{solv,MM/PB}(q^{vac,conf.dep}) \quad (5)$$

Similar estimates can be obtained using the MM/SC solvation model.[33] Because PB and SC models rely on different approximations (grid vs charge distributed over cavity surface, respectively), a comparison of their results will help us to assess the errors relating to these approximations. It should be noted that only the intermolecular solute−solvent contribution (ΔG_{Sv}^{CDC}) can be obtained in this way. The intramolecular solute contribution (ΔG_{Su}^{CDC}) is more challenging because it is not well represented by the internal Coulombic energy of the solute as calculated by MM. There seems to be no practical way of obtaining a QM-based estimate of the CDC terms because there is no straightforward procedure to compute conformation-independent QM energies. However, knowing the internal contribution is not critical, because it is automatically included in the derived torsion parameters, and only ΔG_{Sv}^{CDC} contributes to the $\Delta\Delta G^{solv,QM-MM}$ term which is being analyzed here.

Figure 5 shows both MM/PB and MM/SC estimates of the ΔG_{Sv}^{CDC} term as a function of the torsion angle χ. The

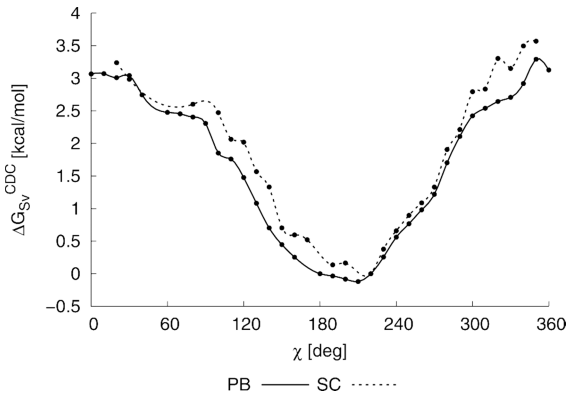

Figure 5. The solvent response to conformation charge dependence (ΔG_{Sv}^{CDC}) as a function of the torsion angle χ, estimated using the MM/PB (full line) and MM/SC (dotted line) models. Both curves are offset relative to the energy for χ = 210° (corresponding to the *anti* region in A-RNA).

similarity of profiles determined from the MM/PB and MM/SC computations suggests that the magnitude of this term is correctly estimated by both. Its magnitude is quite large (up to 3.5 kcal/mol) and significantly contributes to the relative energies of the important regions: the *anti* region around 210° is stabilized by about 2.5 kcal/mol with respect to the *syn* region around 75° and by almost 1 kcal/mol with respect to the high-*anti* region around 250° that is typical for B-DNA. Interestingly, the shape and magnitude of the curve in Figure 5 resembles that of the difference between the QM and PB solvation models shown in Figure 4 (red curve). This implies that the solvent's response to conformation-dependent charges may be an important component of the $\Delta\Delta G^{solv,QM-MM}$ term. However, these results are still based on conformation-dependent charges derived in vacuo. Solute polarization may modify this picture, as discussed below.

4.3. Magnitude of the Solute Polarization. Effects relating to solute polarization, both intramolecular and intermolecular, can be estimated quite accurately by decomposing the QM/SCRF calculation.[48] The contribution of solute−solvent polarization to the solvation Gibbs energy, $\Delta G^{SSP,QM}$, can be calculated as the difference between the full solvation energy (polarized solute−solvent) and the solvation Gibbs energy of the in vacuo wave function (unpolarized solute−solvent), as noted in eq 6a. The intramolecular (solute) and intermolecular (solute−solvent) components are calculated according to eqs 6b and 6c, respectively.

$$\Delta G^{SSP,QM} = \langle\Psi(f)|H + V(f)/2|\Psi(f)\rangle - \langle\Psi(0)|H + V(0)/2|\Psi(0)\rangle \quad (6a)$$

$$\Delta G_{Su}^{SSP,QM} = \langle\Psi(f)|H|\Psi(f)\rangle - \langle\Psi(0)|H|\Psi(0)\rangle \quad (6b)$$

$$\Delta G_{Sv}^{SSP,QM} = \Delta G^{SSP,QM} - \Delta G_{Su}^{SSP,QM} \quad (6c)$$

Here, $\Psi(0)$ is the solute wave function in a vacuum, $\Psi(f)$ is the wave function of the solute polarized by the solvent, $H + V(f)/2$ is the Hamiltonian including the self-consistent solvent reaction field, and $H + V(0)/2$ is the Hamiltonian including the reaction field induced by the vacuum charge distribution of the solute.

Another way of estimating the ΔG^{SSP} term involves force field calculations using two different charge sets, one for the nonpolarized solute in vacuo ($q^{vac,conf.dep}$) and the other for the polarized solute in solution ($q^{pol,conf.dep}$; derived from the wave function obtained from a QM/SCRF calculation). Here, the MM/PB method can provide the ΔG_{Sv}^{SSP} term (eq 7), and the semiclassical approach can estimate both the ΔG_{Sv}^{SSP} and ΔG_{Su}^{SSP} terms. For more details, see refs 45 and 33; the solvation components considered in this work relate to those described in ref 33 as follows: $\Delta G^{upSu-Sv} = \Delta G_{ele}^{0}$, $\Delta G^{SSP} = \Delta G_{pol}$, $\Delta G_{Su}^{SSP} = \Delta G_{dis}$, and $\Delta G_{Sv}^{SSP} = \Delta G_{stab}$.

$$\Delta G_{Sv}^{SSP,PB} = \Delta G^{solv,MM/PB}(q^{pol,conf.dep.}) - \Delta G^{solv,MM/PB}(q^{vac,conf.dep}) \quad (7)$$

Results obtained using the three methods listed above are compared in Figure 6, where the reference QM/SCRF values are shown in black and the estimates obtained with the MM/PB and MM/SC models are shown in dark blue and light blue, respectively. The $\Delta G^{SSP,QM}$ term is represented by the full lines

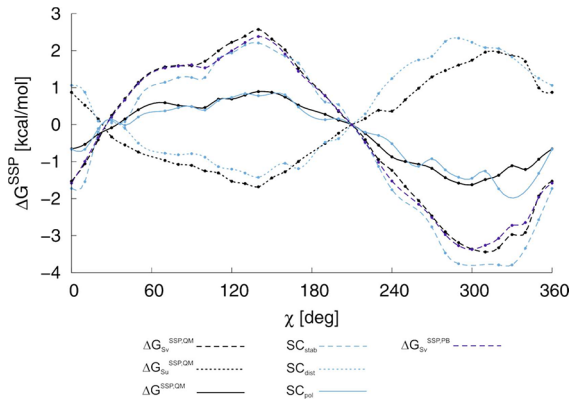

Figure 6. The contributions of solute−solvent polarization to the solvation energy estimated using the QM/SCRF (black), MM/PB (dark blue), and MM/SC (light blue) models. The sum of the intermolecular components (ΔG_{Sv}^{SSP}, dashed lines) and the intramolecular components (ΔG_{Su}^{SSP}, dotted lines) gives the total ΔG^{SSP} (full lines). All curves are offset relative to the energy for χ = 210° (corresponding to the *anti* region in A-RNA).

and its components by dashed ($\Delta G_{Sv}^{SSP,QM}$) and dotted ($\Delta G_{Su}^{SSP,QM}$) lines. Remarkably, the three solvation models provide very similar results, bolstering our confidence in the force-field-based estimates of the solvation energy components, including the estimates of the ΔG^{CDC} terms given in the preceding section.

We now compare the magnitude of the SSP and CDC effects. The solvent response to charge polarization varies over more than 5 kcal/mol, but about half of this change in energy is canceled out by the intramolecular polarization of the solute, ΔG_{Su}^{SSP}. The net contribution of polarization to the χ dependence of the solvation energy thus varies by around 2 kcal/mol. Although this is less than the effects due to conformation charge dependence, it is still a fairly large contribution relative to the amplitude of the torsion profile. Therefore, it seems that both CDC and SSP contributions are significant and should not be neglected.

4.4. Can Solute Polarization and Conformation Charge Dependence Explain the Difference Between the MM/PB and QM/SCRF Models? We hypothesized that the solute−solvent polarization and CDC solvation energy were the most important contributors to the $\Delta\Delta G^{solv,QM-MM}$ term. With the data discussed above, it becomes possible to compare all these quantities in one plot. Figure 7 shows the

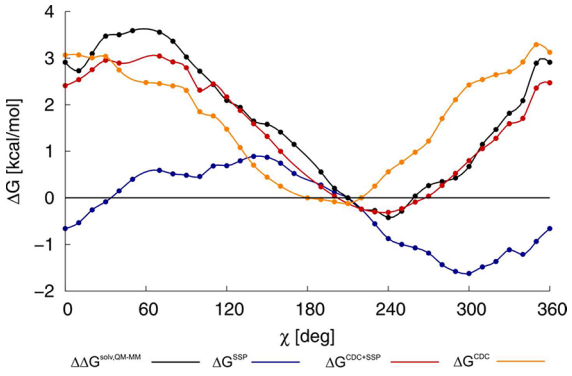

Figure 7. The $\Delta\Delta G^{solv,QM-MM}$ difference (black) and the contributions of the conformation-dependent charges to solvation (ΔG^{CDC}, orange), solute−solvent polarization (ΔG^{SSP}, blue), and their sum (red). All curves are offset relative to the energy for χ = 210° (corresponding to the *anti* region in A-RNA).

ΔG^{SSP} term estimated using the QM/SCRF method (blue), the ΔG^{CDC} term estimated by MM/PB calculations (orange), and their sum, $\Delta G^{CDC+SSP}$ (red), which should be compared to the $\Delta\Delta G^{solv,QM-MM}$ difference (black). It appears that the CDC contribution alone is very similar in shape to the $\Delta\Delta G^{solv,QM-MM}$ term and seems to be the most important term for the χ torsion solvation energies. The contribution of ΔG^{SSP} is somewhat smaller, and when added to the ΔG^{CDC} contribution, it improves the overall agreement with $\Delta\Delta G^{solv,QM-MM}$. Clearly, most of the difference between the MM/PB and QM/SCRF models can be explained by solute−solvent polarization and the solvent's response to variation in the solute's charge distribution stemming from conformational changes. Note that these two terms represent sizable and physically meaningful contributions that are neglected when using torsion parameters derived in vacuo. It therefore seems that including the $\Delta\Delta G^{solv,QM-MM}$ ($\approx \Delta G^{SSP} + \Delta G^{CDC}$) correction in torsion parameters intended for use in solvents seems to be reasonable and justified.

4.5. Can HF/RESP Charges Mimic the Effect of Solvation on Torsion Profiles? Nonpolarizable force fields use prepolarized charges to mimic solute−solvent polarization. For instance, ff94 uses the HF/6-31G* RESP charges, which overestimate dipole moments, and ff03 uses solvent-prepolarized charges,[15] which are supposed to mimic the effect of solute−solvent polarization. It would be interesting to see how well the prepolarized charges capture the conformation dependence of the solvation energy. Figure 8 shows the total

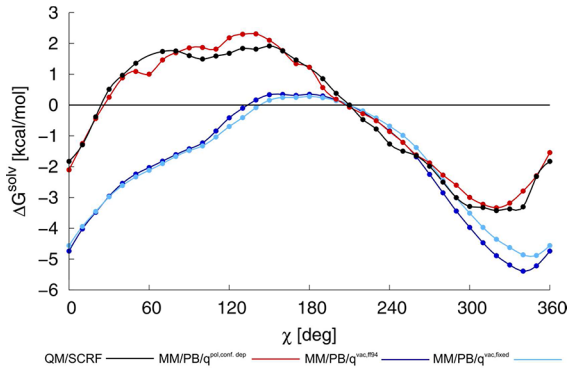

Figure 8. The total solvation energy of deoxyribonucleoside as a function of the torsion angle χ. The reference QM/SCRF curve (black) is compared to the MM/PB solvation energies obtained using the ff94 point charges (dark blue), vacuum-derived charges, $q^{vac,fixed}$ (light blue), and polarized conformation-dependent charges, $q^{pol,conf.dep}$ (red). All curves are offset relative to the energy for χ = 210° (corresponding to the *anti* region in A-RNA).

solvation energies calculated using different models as a function of the torsion angle χ. All results are normalized to χ = 210° (*anti*, A-DNA and A-RNA forms). The QM/SCRF curve ($\Delta G^{solv,QM}$) is our best estimate of the solvation energy (black line). The solvation energy obtained using fixed vacuum charges ($q^{vac,fixed}$) in the MM/PB model ($\Delta G^{upSu-Sv}$) is shown by the light blue line. The MM/PB solvation energy obtained using prepolarized force field charges (q^{ff94}) is shown in dark blue. Finally, our MM/PB-based estimate of the full solvation energy using polarized and conformation-dependent charges ($q^{pol,conf.dep.}$) is shown in red. This estimate is calculated as $\Delta G^{solv} = \Delta G^{upSu-Sv} + \Delta G^{CDC} + 1/2\Delta G_{Sv}^{SSP}$, where the 1/2 factor in the last term comes from eq 6c, in which we approximate $\Delta G_{Su}^{SSP} \approx -1/2\Delta G_{Sv}^{SSP}$ (see also Figure 6 and refs 33 and 45). The agreement between the QM/SCRF calculations and the MM/PB calculations using the $q^{pol,conf.dep}$ charges seems to be very good. In contrast, the MM/PB calculations using the fixed charges derived in vacuo give results that deviate substantially from the reference curve. Interestingly, the same holds for the prepolarized ff94 charges, which give very similar results to those obtained with the in vacuo derived charges. This indicates that using prepolarized charges such as HF-6-31G*/RESP charges or those of Duan et al. does not guarantee an accurate description of the conformational dependence of the solvation energy and can generate significant errors.

Note that Figure 8 only shows the variation of the solvation energy with the χ angle. The absolute magnitudes of the solvation energies determined using the ff94 and $q^{vac,fixed}$ charges differ (on average, they are −25.0 and −18.6 kcal/mol, respectively). However, it should be emphasized that the absolute magnitude of the $\Delta\Delta G^{solv,QM-MM}$ term is not relevant

dx.doi.org/10.1021/ct3001987 | J. Chem. Theory Comput. 2012, 8, 3232−3242

for us, because the derived parameters are only sensitive to the way it varies as a function of the torsion angle. The absolute differences between the QM/SCRF and MM/PB models are therefore unimportant in this derivation.

4.6. Incorporating Solvation Effects into Torsion Parameters. One way of incorporating the above-described conformation-dependent solvation effects in the dihedral torsion parameters is to apply eq 2. In this method, both QM and the MM calculations are carried out in continuum solvent. This means that most of the solvation energy ($\Delta G^{upSu-Sv}$) will cancel out and only the desirable solvation contributions ($\Delta G^{SSP} + \Delta G^{CDC} \approx \Delta\Delta G^{solv,QM-MM}$) become an integral part of the torsion potential. One potential concern regarding this scheme stems from its reliance on perfect cancellation of the unpolarized solute−solvent energies described by the different solvent models (see also eq 4). If this cancellation is imperfect, the corresponding difference will appear in the resulting parameters. Therefore, one should make sure that the errors arising from this assumption of cancellation are negligible, or at least much smaller than the desirable effects one wants to address. The extent to which cancellation of the $\Delta G^{upSu-Sv}$ terms can be achieved is partly dictated by the nature of the methods used (e.g., the use of the wave function rather than point charges) and partly by the radii used and, to a lesser extent, the cavity construction algorithm. In this work, we used the same radii for both QM/SCRF and MM/PB calculations to ensure consistency. The $\Delta G^{upSu-Sv}$ energies calculated using different methods are shown in Figure 9. The value of the

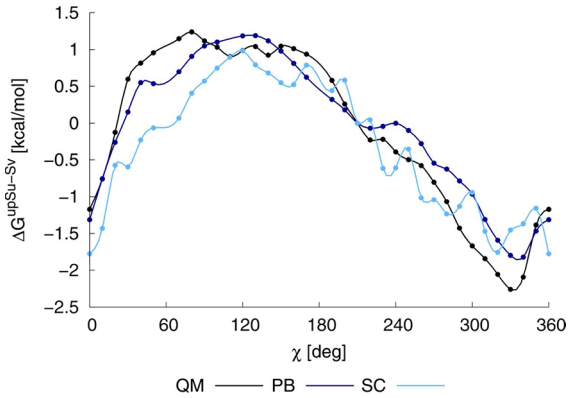

Figure 9. Unpolarized solute−solvent solvation energies ($\Delta G^{upSu-Sv}$) estimated using the QM/SCRF (black) method and the MM/PB (dark blue) and MM/SC (light blue) models with conformation-dependent vacuum charges ($q^{vac,conf.dep}$). All curves are offset relative to the energy for $\chi = 210°$ (corresponding to the *anti* region in A-RNA).

$\Delta G^{upSu-Sv}$ term was obtained directly from the QM/SCRF calculations (results plotted in black), and the conformation-dependent in vacuo charges, $q^{vac,conf.dep}$, were used for the MM/PB and MM/SC calculations (whose results are plotted in dark and light blue, respectively).

Figure 9 shows that all three models provide very similar results. In particular, the differences between the QM/SCRF and MM/PB models are much smaller than the magnitude of the $\Delta\Delta G^{solv,QM-MM}$ correction term (almost 4 kcal/mol). This indicates that our correction, although being approximate, primarily represents desirable effects. Thus, the improvements from inclusion of the missing solvation effects into the χ potential should outweigh the shortcomings of the solvent models used in derivation.

There are of course other questions connected with use of continuum solvent models that may be of concern. One is the choice of the relative permittivity value. Here, we used $\varepsilon_r = 78.4$ (i.e., the relative permittivity of water) to simulate the very polar environment surrounding the strongly hydrated nucleic acids. However, when torsions are derived for other environments or complex systems, it may be necessary to use a different value for the relative permittivity. Unfortunately, this problem is inherent to pairwise additive force field models.

Finally, it should be noted that the torsion parameters should in general contain only intramolecular terms, but the $\Delta G^{CDC+SSP}$ energy also incorporates intermolecular terms (solvation energy − interaction with solvent). However, because it is not possible to model these solvation terms explicitly within the framework of classical nonpolarizable discrete solvents, it should still be advantageous to incorporate them into the torsion parameters, which may then be understood as an "effective" potential.

In conclusion, the suggested methodology makes it possible to incorporate corrections for otherwise neglected solvation effects into dihedral torsion parameters. The derived parameters are expected to yield better results than those obtained using conventional methods, as demonstrated with the recent RNA parmχ_{OL3} parametrization.[3]

4.7. The Performance of the Derived Parameters in MD Simulations. In a previous work,[3] we derived new χ torsion parameters (named χ_{OL}) using the solvation procedure described herein. These parameters have been incorporated into the ff10 force field in the Amber software package, where they are denoted χ_{OL3}. In the same work and at the same level of theory, we also derived a set of in vacuo parameters, χ_{vac}. Comparing the performance of these two parameter sets in MD simulations will help us to demonstrate the importance of the solvation effects discussed in this work. Figure 4 shows that solvation effects strongly influence several features of the χ torsion potential as they alter barrier heights, change the shape of the *anti* minimum, and affect the relative energy of the *anti* and *syn* minima. Indeed, MD simulations carried out using both parameter sets seem to reflect these differences. Our recent MD simulations of the GAGA tetraloop showed that the in-solvent derived χ_{OL3} parameters yielded stable structures that were close to the X-ray reference.[1] However, simulations using the in vacuo derived χ_{vac} and ff99bsc0 parameters (this work) resulted in rapid degradation to a ladder-like structure within 15 ns, which is even more rapid than the degradation observed with the ff99 based force field (36 ns with ff99bsc0 and 20 ns with ff99, see ref 1). The propensity to form ladder-like structures thus seems to correlate with the extent of *anti*/high-*anti* destabilization, as discussed in ref 3 (see Table 2 in the cited study). Because these three simulations differ only in the χ parameters used (the ff99bsc0 force field was used in all three cases), the small differences in the shape of the *anti*/high-*anti* minimum introduced by the solvation correction in χ_{OL3} are clearly sufficient to stabilize MD simulations of RNA structures.

Another sequence simulated with both χ_{OL3} and χ_{vac} was a canonical RNA decamer 1QC0′ (ff99bsc0, 100 ns run, for details see ref 9). In this case, the results obtained with parameters derived in vacuo resembled those achieved in the original ff99bsc0 simulation, except that the major groove width was somewhat greater and the RMSD values were a little worse with χ_{vac}. The similarity of the ff99bsc0 and ff990bsc0χ_{vac} performance is not surprising, since the shape of the original ff99bsc0 torsion potential more closely resembles that of the

parameters derived in vacuo than that of the parameters derived in solution. Both ff99bsc0 and ff99bsc0χ_{vac} destabilize the *anti* region with respect to the high-*anti* region and provide more stability to the *syn* region than the in-solvent derived parameters. This is probably because, although the original ff99 force field was not directly derived from the in vacuo QM torsion potential, some in vacuo QM calculations were considered during its derivation.[13]

Upon suggestion of a reviewer we also fitted a third set of χ parameters, $\chi_{wat,full\text{-}solv}$, using the full SCRF (COSMO) solvation energy ($E^{QM,vac} + \Delta G^{solv,QM/SCRF}$) as a target (similar approach was used in ref 15). This means that our target for fitting was $E^{QM,vac} + \Delta G^{solv,QM/SCRF}$, not $E^{QM,vac} + \Delta\Delta G^{solv,QM-MM}$ as in eq 2. The remaining details of fitting were the same as for χ_{OL3}[3]; therefore, any differences can be ascribed to the use of full solvation energy as a target. The most important difference introduced by fitting the full solvation energy is the overstabilization of the high-*anti* region above 240° (see Figure S2 in Supporting Information), which should lead to stabilization of the ladder-like structures as described in ref 3. Indeed, our molecular dynamics simulations confirmed transition to the ladder like structure at the nanosecond time scale (1 to 5 ns in several simulations of the 1RNA tetradecamer, data not shown); therefore, $\chi_{wat,full\text{-}solv}$ parameters were not studied further. These findings demonstrate the sensitivity of structural details of RNA to apparently minor differences in the parameters for the torsion angle χ.

5. CONCLUSIONS

An alternative method to derive torsion parameters for MD simulations is examined. The key point of the method is that it includes conformation-dependent solvation effects that are neglected when torsion parameters are derived in vacuo and are not covered by the solvent models used in MD simulations. We find that the two most important contributions to the variation in the solvation energy due to torsion rotation are (i) the solvent's response to conformation-dependent variation in the solute's charge distribution and (ii) conformation-dependent solute−solvent polarization. The magnitude of these two effects was investigated for the χ torsion angle using a modified cytosine deoxyribonucleoside as a model. Both effects were shown to be substantial and to significantly modify the shape of the χ torsion profile, namely, the relative stability of the *syn* and *anti* regions and of the *anti* and high-*anti* regions. It is likely that similar errors will result for other polar molecules.

A viable procedure for incorporating the missing solvation effects into the torsion angle parametrization is based on the difference between QM/SCRF and MM/PB continuum solvation energies (for a detailed description of the torsion derivation including geometry relaxation effects, see ref 3). It is shown that this method ensures that only those solvation effects that cannot be described by the solvent model used in the MD simulation become incorporated into the torsion parameters and that double counting of solvation contributions is avoided. The derived torsion parameters can be used for simulations with any standard nonpolarizable explicit solvent model and even with implicit solvent models.

As shown in a separate publication, the Zgarbova et al. χ_{OL3} parameters derived with the inclusion of conformation-dependent solvent effects eliminate a recently identified and important artifact in MD simulations of RNA hairpin loops, namely, the formation of undesirable ladder-like structures.[1] In addition, the method yields an improved description of the position and relative energy of the *syn* minimum and the torsion barrier heights.[1,3]

We suggest that accounting for solvation related errors is likely to provide consistently better torsion parameters than the conventional in vacuo parametrization approach and may help to systematically reduce errors in future force fields. While these parameters will still require extensive testing in simulations (and probably some subsequent adjustment), they should provide a better basis for development efforts than their "in vacuo" counterparts.

■ ASSOCIATED CONTENT

Supporting Information

In vacuo comparison of QM χ torsion profile with χ_{OL3} MM profile and with QM profile calculated in continuum solvent. This material is available free of charge via the Internet at http://pubs.acs.org.

■ AUTHOR INFORMATION

Corresponding Author

*E-mail: petr.jurecka@upol.cz.

Notes

The authors declare no competing financial interest.

■ ACKNOWLEDGMENTS

This work was supported by grants P208/10/1742 (P.J.), 203/09/H046 (P.J., M.O., J.S., and M.Z.), 203/09/1476 (J.S.), P208/11/1822 (J.S.), P208/12/1878 (J.S., M.O., P.J., M.Z.), and P305/12/G03 (J.S.) from the Grant Agency of the Czech Republic. Further funding was provided by the Operational Program Research and Development for Innovations of the European Regional Development Fund via projects CZ.1.05/2.1.00/03.0058 and CZ.1.07/2.3.00/20.0017 administered by the Ministry of Education, Youth and Sports of the Czech Republic), by the European Regional Development Fund via project CZ.1.05/1.1.00/02.0068 of CEITEC—the Central European Institute of Technology, by the Spanish Ministry of Innovation and Science (F.J.L.; SAF2011-27642), and the Generalitat de Catalunya (F.J.L.; 2009SGR249). Finally, M.Z. acknowledges the HPC-Europa2 project (project no. 228398) with the support of the European Community—Research Infrastructure Action of the FP7 for providing access to supercomputing resources at the Barcelona Supercomputer Center.

■ REFERENCES

(1) Banáš, P.; Hollas, D.; Zgarbova, M.; Jurecka, P.; Orozco, M.; Cheatham, T.; Sponer, J.; Otyepka, M. *J. Chem. Theory Comput.* **2010**, *6* (12), 3836−3849.

(2) Ditzler, M. A.; Otyepka, M.; Sponer, J.; Walter, N. G. *Acc. Chem. Res.* **2010**, *43* (1), 40−47.

(3) Zgarbova, M.; Otyepka, M.; Sponer, J.; Mladek, A.; Banas, P.; Cheatham, T. E., 3rd; Jurecka, P. *J. Chem. Theory Comput.* **2011**, *7* (9), 2886−2902.

(4) Schneider, B.; Moravek, Z.; Berman, H. M. *Nucleic Acids Res.* **2004**, *32* (5), 1666−1677.

(5) Svozil, D.; Kalina, J.; Omelka, M.; Schneider, B. *Nucleic Acids Res.* **2008**, *36* (11), 3690−3706.

(6) Cheatham, T. E.; Cieplak, P.; Kollman, P. A. *J. Biomol. Struct. Dyn.* **1999**, *16* (4), 845−862.

(7) Foloppe, N.; MacKerell, A. D. *J. Comput. Chem.* **2000**, *21* (2), 86−104.

(8) Foloppe, N.; Hartmann, B.; Nilsson, L.; MacKerell, A. D. *Biophys. J.* **2002**, *82* (3), 1554−1569.

(9) Perez, A.; Marchan, I.; Svozil, D.; Sponer, J.; Cheatham, T. E.; Laughton, C. A.; Orozco, M. *Biophys. J.* **2007**, *92* (11), 3817−3829.
(10) Ode, H.; Matsuo, Y.; Neya, S.; Hoshino, T. *J. Comput. Chem.* **2008**, *29* (15), 2531−2542.
(11) Yildirim, I.; Stern, H. A.; Kennedy, S. D.; Tubbs, J. D.; Turner, D. H. *J. Chem. Theory Comput.* **2010**, *6* (5), 1520−1531.
(12) Cornell, W. D.; Cieplak, P.; Bayly, C. I.; Gould, I. R.; Merz, K. M.; Ferguson, D. M.; Spellmeyer, D. C.; Fox, T.; Caldwell, J. W.; Kollman, P. A. *J. Am. Chem. Soc.* **1995**, *117* (19), 5179−5197.
(13) Wang, J. M.; Cieplak, P.; Kollman, P. A. *J. Comput. Chem.* **2000**, *21* (12), 1049−1074.
(14) Foloppe, N.; MacKerell, A. D. *Biophys. J.* **1999**, *76* (6), 3206−3218.
(15) Duan, Y.; Wu, C.; Chowdhury, S.; Lee, M. C.; Xiong, G. M.; Zhang, W.; Yang, R.; Cieplak, P.; Luo, R.; Lee, T.; Caldwell, J.; Wang, J. M.; Kollman, P. *J. Comput. Chem.* **2003**, *24* (16), 1999−2012.
(16) Orozco, M.; Bachs, M.; Luque, F. J. *J. Comput. Chem.* **1995**, *16* (5), 563−575.
(17) Luque, F. J.; Bachs, M.; Aleman, C.; Orozco, M. *J. Comput. Chem.* **1996**, *17* (7), 806−820.
(18) Luque, F. J.; Zhang, Y.; Aleman, C.; Bachs, M.; Gao, J.; Orozco, M. *J. Phys. Chem.* **1996**, *100* (10), 4269−4276.
(19) Curutchet, C.; Orozco, M.; Luque, F. J. *J. Comput. Chem.* **2001**, *22* (11), 1180−1193.
(20) Cances, E.; Mennucci, B.; Tomasi, J. *J. Chem. Phys.* **1997**, *107* (8), 3032−3041.
(21) Mennucci, B.; Cances, E.; Tomasi, J. *J. Phys. Chem. B* **1997**, *101* (49), 10506−10517.
(22) Cances, E.; Mennucci, B. *J. Math. Chem.* **1998**, *23* (3−4), 309−326.
(23) Klamt, A.; Schuurmann, G. *J. Chem. Soc., Perkin Trans. 2* **1993**, No. 5, 799−805.
(24) Klamt, A. *J. Phys. Chem.* **1995**, *99* (7), 2224−2235.
(25) Klamt, A.; Jonas, V.; Burger, T.; Lohrenz, J. C. W. *J. Phys. Chem. A* **1998**, *102* (26), 5074−5085.
(26) Marenich, A. V.; Cramer, C. J.; Truhlar, D. G. *J. Phys. Chem. B* **2009**, *113* (18), 6378−6396.
(27) MacKerell, A. D.; Banavali, N. K. *J. Comput. Chem.* **2000**, *21* (2), 105−120.
(28) Bosch, D.; Foloppe, N.; Pastor, N.; Pardo, L.; Campillo, M. *THEOCHEM* **2001**, *537*, 283−305.
(29) Banas, P.; Jurecka, P.; Walter, N. G.; Sponer, J.; Otyepka, M. *Methods* **2009**, *49* (2), 202−216.
(30) Mlynsky, V.; Banas, P.; Hollas, D.; Reblova, K.; Walter, N. G.; Sponer, J.; Otyepka, M. *J. Phys. Chem. B* **2010**, *114* (19), 6642−6652.
(31) Sklenovsky, P.; Florova, P.; Banas, P.; Reblova, K.; Lankas, F.; Otyepka, M.; Sponer, J. *J. Chem. Theory Comput.* **2011**, *7* (9), 2963−2980.
(32) Case, D. A.; Darden, T. A.; Chetham, T. E., III; Simmerling, C. E.; Wang, J.; Duke, R. E.; Luo, R.; Walker, R. C.; Zhang, W.; Merz, K. M.; Roberts, B. P.; Wang, B.; Hayik, S.; Roitberg, A.; Seabra, G.; Kolossvary, I.; Wong, K. F.; Paesani, F.; Vanicek, J.; Liu, J.; Wu, X.; Brozell, S. R.; Steinbrecher, T.; Gohlke, H.; Cai, Q.; Ye, X.; Wang, J.; Hsieh, M. J.; Cui, G.; Roe, D. R.; Mathews, D. H.; Seetin, M. G.; Sagui, C.; Babin, V.; Luchko, T.; Gusarov, V.; Kovalenko, A.; Kollmann, P. A. *AMBER 11*, University of California: San Francisco, CA, 2010.
(33) Luque, F. J.; Orozco, M. *J. Phys. Chem. B* **1997**, *101* (28), 5573−5582.
(34) Perdew, J. P.; Burke, K.; Ernzerhof, M. *Phys. Rev. Lett.* **1996**, *77* (18), 3865−3868.
(35) Krishnan, R.; Binkley, J. S.; Seeger, R.; Pople, J. A. *J. Chem. Phys.* **1980**, *72* (1), 650−654.
(36) Clark, T.; Chandrasekhar, J.; Spitznagel, G. W.; Schleyer, P. V. *J. Comput. Chem.* **1983**, *4* (3), 294−301.
(37) Frisch, M. J.; Pople, J. A.; Binkley, J. S. *J. Chem. Phys.* **1984**, *80* (7), 3265−3269.
(38) Gill, P. M. W.; Johnson, B. G.; Pople, J. A. *J. Chem. Phys.* **1992**, *96* (9), 7178−7179.
(39) Ahlrichs, R.; Bar, M.; Haser, M.; Horn, H.; Kolmel, C. *Chem. Phys. Lett.* **1989**, *162* (3), 165−169.
(40) Weigend, F.; Häser, M. *Theor. Chem. Acc.* **1997**, *97* (1−4), 331−340.
(41) Klamt, A.; Eckert, F.; Diedenhofen, M. *J. Phys. Chem. B* **2009**, *113* (14), 4508−4510.
(42) Klamt, A.; Diedenhofen, M. *J. Comput.-Aided Mol. Des.* **2010**, *24* (4), 357−360.
(43) Frisch, M. J.; Trucks, G. W.; Schlegel, H. B.; Scuseria, G. E.; Robb, M. A.; Cheeseman, J. R.; Montgomery, J. A., Jr.; Vreven, T.; Kudin, K. N.; Burant, J. C.; Millam, J. M.; Iyengar, S. S.; Tomasi, J.; Barone, V.; Mennucci, B.; Cossi, M.; Scalmani, G.; Rega, N.; Petersson, G. A.; Nakatsuji, H.; Hada, M.; Ehara, M.; Toyota, K.; Fukuda, R.; Hasegawa, J.; Ishida, M.; Nakajima, T.; Honda, Y.; Kitao, O.; Nakai, H.; Klene, M.; Li, X.; Knox, J. E.; Hratchian, H. P.; Cross, J. B.; Bakken, V.; Adamo, C.; Jaramillo, J.; Gomperts, R.; Stratmann, R. E.; Yazyev, O.; Austin, A. J.; Cammi, R.; Pomelli, C.; Ochterski, J. W.; Ayala, P. Y.; Morokuma, K.; Voth, G. A.; Salvador, P.; Dannenberg, J. J.; Zakrzewski, V. G.; Dapprich, S.; Daniels, A. D.; Strain, M. C.; Farkas, O.; Malick, D. K.; Rabuck, A. D.; Raghavachari, K.; Foresman, J. B.; Ortiz, J. V.; Cui, Q.; Baboul, A. G.; Clifford, S.; Cioslowski, J.; Stefanov, B. B.; Liu, G.; Liashenko, A.; Piskorz, P.; Komaromi, I.; Martin, R. L.; Fox, D. J.; Keith, T.; Al-Laham, M. A.; Peng, C. Y.; Nanayakkara, A.; Challacombe, M.; Gill, P. M. W.; Johnson, B.; Chen, W.; Wong, M. W.; Gonzalez, C.; Pople, J. A. *Gaussian 03*, revision D.02; Gaussian, Inc.: Wallingford, CT, 2004.
(44) Case, D. A.; Darden, T. A.; Chetham, T. E., III; Simmerling, C. E.; Wang, J.; Duke, R. E.; Luo, R.; Crowley, M.; Walker, R. C.; Zhang, W.; Merz, K. M.; Wang, B.; Hayik, S.; Roitberg, A.; Seabra, G.; Kolossvary, I.; Wong, K. F.; Paesani, F.; Vanicek, J.; Wu, X.; Brozell, S.; Steinbrecher, H.; Gohlke, H.; Yang, L.; Tan, C.; Mongan, J.; Hornak, V.; Cui, G.; Mathews, D. H.; Seetin, M. G.; Sagui, C.; Babin, V.; Kollmann, P. A. *AMBER 10*; University of California: San Francisco, CA, 2008.
(45) Luque, F. J.; Bofill, J. M.; Orozco, M. *J. Chem. Phys.* **1995**, *103* (23), 10183−10191.
(46) Bayly, C. I.; Cieplak, P.; Cornell, W. D.; Kollman, P. A. *J. Phys. Chem.* **1993**, *97* (40), 10269−10280.
(47) Reynolds, C. A.; Essex, J. W.; Richards, W. G. *J. Am. Chem. Soc.* **1992**, *114* (23), 9075−9079.
(48) Luque, F. J.; Curutchet, C.; Munoz-Muriedas, J.; Bidon-Chanal, A.; Soteras, I.; Morreale, A.; Gelpi, J. L.; Orozco, M. *Phys. Chem. Chem. Phys.* **2003**, *5* (18), 3827−3836.